# Inhibition of MCU forces extramitochondrial adaptations governing physiological and pathological stress responses in heart

Tyler P. Rasmussen[a,b,1], Yuejin Wu[c,1], Mei-ling A. Joiner[b], Olha M. Koval[b], Nicholas R. Wilson[c], Elizabeth D. Luczak[c], Qinchuan Wang[c], Biyi Chen[b], Zhan Gao[b], Zhiyong Zhu[b], Brett A. Wagner[d], Jamie Soto[b], Michael L. McCormick[d], William Kutschke[b], Robert M. Weiss[b], Liping Yu[e,f], Ryan L. Boudreau[b], E. Dale Abel[b,g], Fenghuang Zhan[b], Douglas R. Spitz[d], Garry R. Buettner[d], Long-Sheng Song[b], Leonid V. Zingman[b], and Mark E. Anderson[c,2]

[a]Department of Molecular Physiology and Biophysics, University of Iowa Carver College of Medicine, Iowa City, IA 52242; [b]Department of Internal Medicine, University of Iowa Carver College of Medicine, Iowa City, IA 52242; [c]Department of Medicine, The Johns Hopkins University School of Medicine, Baltimore, MD 21287; [d]Free Radical and Radiation Biology Program, University of Iowa Carver College of Medicine, Iowa City, IA 52242; [e]Department of Biochemistry, University of Iowa Carver College of Medicine, Iowa City, IA 52242; [f]Nuclear Magnetic Resonance Core Facility, University of Iowa Carver College of Medicine, Iowa City, IA 52242; and [g]Fraternal Order of Eagles Diabetes Research Center, University of Iowa Carver College of Medicine, Iowa City, IA 52242

Edited by Tullio Pozzan, University of Padova, Padova, Italy, and approved June 1, 2015 (received for review March 12, 2015)

**Myocardial mitochondrial $Ca^{2+}$ entry enables physiological stress responses but in excess promotes injury and death. However, tissue-specific in vivo systems for testing the role of mitochondrial $Ca^{2+}$ are lacking. We developed a mouse model with myocardial delimited transgenic expression of a dominant negative (DN) form of the mitochondrial $Ca^{2+}$ uniporter (MCU). DN-MCU mice lack MCU-mediated mitochondrial $Ca^{2+}$ entry in myocardium, but, surprisingly, isolated perfused hearts exhibited higher $O_2$ consumption rates (OCR) and impaired pacing induced mechanical performance compared with wild-type (WT) littermate controls. In contrast, OCR in DN-MCU–permeabilized myocardial fibers or isolated mitochondria in low $Ca^{2+}$ were not increased compared with WT, suggesting that DN-MCU expression increased OCR by enhanced energetic demands related to extramitochondrial $Ca^{2+}$ homeostasis. Consistent with this, we found that DN-MCU ventricular cardiomyocytes exhibited elevated cytoplasmic [$Ca^{2+}$] that was partially reversed by ATP dialysis, suggesting that metabolic defects arising from loss of MCU function impaired physiological intracellular $Ca^{2+}$ homeostasis. Mitochondrial $Ca^{2+}$ overload is thought to dissipate the inner mitochondrial membrane potential ($\Delta\Psi m$) and enhance formation of reactive oxygen species (ROS) as a consequence of ischemia-reperfusion injury. Our data show that DN-MCU hearts had preserved $\Delta\Psi m$ and reduced ROS during ischemia reperfusion but were not protected from myocardial death compared with WT. Taken together, our findings show that chronic myocardial MCU inhibition leads to previously unanticipated compensatory changes that affect cytoplasmic $Ca^{2+}$ homeostasis, reprogram transcription, increase OCR, reduce performance, and prevent anticipated therapeutic responses to ischemia-reperfusion injury.**

myocardium | mitochondrial calcium uniporter | ischemia-reperfusion injury

Entry of $Ca^{2+}$ into the mitochondrial matrix is a central event for $Ca^{2+}$ homeostasis in cardiomyocytes (1) as well as for coordinating fundamental and diverse responses to physiological (2) and pathological stress (3). The paradigm for $Ca^{2+}$ as a physiological second messenger that enhances oxidative phosphorylation to enable fight-or-flight responses but in excess contributes to disease and dysfunction is well established in myocardium (4). The molecular identity of the mitochondrial $Ca^{2+}$ uniporter (MCU) was recently discovered, enabling development of new genetic models to understand the role of MCU in vivo. MCU is an ion channel protein that acts as the primary pathway for $Ca^{2+}$ entry into the mitochondrial matrix (5, 6). Recent findings in global *Mcu*$^{-/-}$ mice (7) suggest that the MCU pathway is dispensable for regulating cellular energy production, except under extreme physiological stress, and for activation of pathways leading to cell death; however, the effect of selective myocardial MCU inhibition is unknown. We developed a new transgenic mouse model with myocardial delimited dominant negative (DN)-MCU protein overexpression to test the role of MCU-mediated $Ca^{2+}$ entry for myocardial physiology and pathological stress.

We tested whether loss of MCU-mediated $Ca^{2+}$ entry substantially alters myocardial energetics. Surprisingly, we found that DN-MCU hearts had a higher oxygen consumption rate (OCR) due, at least in part, to secondary actions on cytoplasmic $Ca^{2+}$ homeostasis. We also found that chronic MCU inhibition failed to protect against myocardial ischemia-reperfusion injury despite reducing generation of reactive oxygen species (ROS). We queried mRNA expression in adult hearts and identified diverse changes in multiple gene pathways induced by DN-MCU

## Significance

Mitochondrial $Ca^{2+}$ is a fundamental signal that allows for adaptation to physiological stress but a liability during ischemia-reperfusion injury in heart. On one hand, mitochondrial $Ca^{2+}$ entry coordinates energy supply and demand in myocardium by increasing the activity of matrix dehydrogenases to augment ATP production by oxidative phosphorylation. On the other hand, inhibiting mitochondrial $Ca^{2+}$ overload is promulgated as a therapeutic approach to preserve myocardial tissue following ischemia-reperfusion injury. We developed a new mouse model of myocardial-targeted transgenic dominant-negative mitochondrial $Ca^{2+}$ uniporter (MCU) expression to test consequences of chronic loss of MCU-mediated $Ca^{2+}$ entry in heart. Here we show that MCU inhibition has unanticipated consequences on extramitochondrial pathways affecting oxygen utilization, cytoplasmic $Ca^{2+}$ homeostasis, physiologic responses to stress, and pathologic responses to ischemia-reperfusion injury.

Author contributions: T.P.R., Y.W., M.-l.A.J., O.M.K., N.R.W., E.D.L., Q.W., B.C., Z.Z., B.A.W., L.Y., R.L.B., E.D.A., F.Z., D.R.S., G.R.B., L.-S.S., L.V.Z., and M.E.A. designed research; T.P.R., Y.W., O.M.K., N.R.W., E.D.L., Q.W., B.C., Z.G., Z.Z., B.A.W., J.S., M.L.M., W.K., L.Y., and L.V.Z. performed research; T.P.R., Y.W., M.-l.A.J., B.C., R.M.W., L.Y., E.D.A., F.Z., D.R.S., G.R.B., L.-S.S., L.V.Z., and M.E.A. contributed new reagents/analytic tools; T.P.R., Y.W., N.R.W., E.D.L., Q.W., B.C., Z.G., B.A.W., J.S., M.L.M., R.M.W., L.Y., R.L.B., E.D.A., D.R.S., L.-S.S., L.V.Z., and M.E.A. analyzed data; and T.P.R., Y.W., and M.E.A. wrote the paper.

The authors declare no conflict of interest.

This article is a PNAS Direct Submission.

Data deposition: The data reported in this paper have been deposited in the Gene Expression Omnibus (GEO) database, www.ncbi.nlm.nih.gov/geo (accession no. GSE62049).

[1]T.P.R. and Y.W. contributed equally to this work.

[2]To whom correspondence should be addressed. Email: mark.anderson@jhmi.edu.

This article contains supporting information online at www.pnas.org/lookup/suppl/doi:10.1073/pnas.1504705112/-/DCSupplemental.

expression. Our findings reveal in vivo physiologic and pathological roles for cardiac MCU and suggest that loss of mitochondrial $Ca^{2+}$ entry increases OCR, elevates cytoplasmic $Ca^{2+}$, and sensitizes extramitochondrial cell death pathways.

## Results

**Increased Myocardial Oxygen Consumption and Reduced Performance in DN-MCU Hearts.** MCU, the pore-forming subunit of the mitochondrial $Ca^{2+}$ uniporter, consists of two transmembrane domains that span the inner mitochondrial membrane and a linker-loop sequence (5, 6). The highly conserved aspartic acid-isoluecine-methionine-glutamic acid motif contains two negatively charged amino acids in the pore-forming linker-loop sequence. DN-MCU with D261Q/E264Q mutations inhibited mitochondrial $Ca^{2+}$ uptake in HeLa cells (6). Based on this information, we developed a myocardial-selective in vivo model of MCU inhibition by transgenic expression of DN-MCU under control of the α-myosin heavy chain (αMHC) promoter (8) (Fig. 1*A*). DN-MCU mice were interbred into a CD1 background, based on evidence that CD1 background is permissive for loss of MCU current (9). DN-MCU mice were born in Mendelian ratios and survived into adulthood. We used a primer set to detect MCU and DN-MCU transcripts and found that the transcript level of *Mcu* was 60-fold higher in transgenic samples (Fig. 1*B*). The Myc-tagged DN-MCU protein was resident only in cardiac mitochondria from DN-MCU transgenic mice (Fig. 1*C*) and was detectable with an MCU antibody that showed markedly increased expression in DN-MCU compared with WT heart lysates (Fig. S1).

Increased mitochondrial $Ca^{2+}$ can enhance oxidative phosphorylation (10). Based on the known relationship between mitochondrial $Ca^{2+}$ and oxidative phosphorylation, we initially hypothesized that DN-MCU hearts lacking $Ca^{2+}$ entry through MCU would have reduced $O_2$ consumption rates (OCR) compared with WT. Contrary to our expectations, unloaded Langendorff-perfused and ventricular paced DN-MCU hearts consumed more $O_2$ at 400 ($P < 0.05$), 600 ($P < 0.01$), and 750 beats/min (bpm) ($P < 0.01$) compared with WT (Fig. 1*D*). OCR was increased in WT between 400 and 600 bpm ($P < 0.01$) but not between 600 and 750 bpm. OCR was increased in DN-MCU between 400 and 600 bpm ($P < 0.0001$) as well as between 600 and 750 bpm ($P < 0.05$). No differences in cardiac morphology or baseline heart rate (Fig. 1*E* and Fig. S2) or in the heart weight: body weight ratios (Fig. 1*F*) were observed. We measured left ventricular (LV) ejection fraction in conscious, unsedated mice and found no difference between groups (Fig. 1*G*). No differences were detected between groups in the mitochondrial injury score (3) (Fig. 1 *H* and *I*), total mitochondrial protein content normalized to heart weight ratios (Fig. 1*J*), or mitochondrial-to-nuclear DNA content (Fig. 1*K*). Additionally, cyclooxygenase 4 (COXIV) protein levels were not different between groups (Fig. S3). These findings suggest that the increase in OCR in DN-MCU hearts was not related to alterations in myocardial or mitochondrial mass or structure but that DN-MCU hearts were less efficient than WT, based on higher OCR.

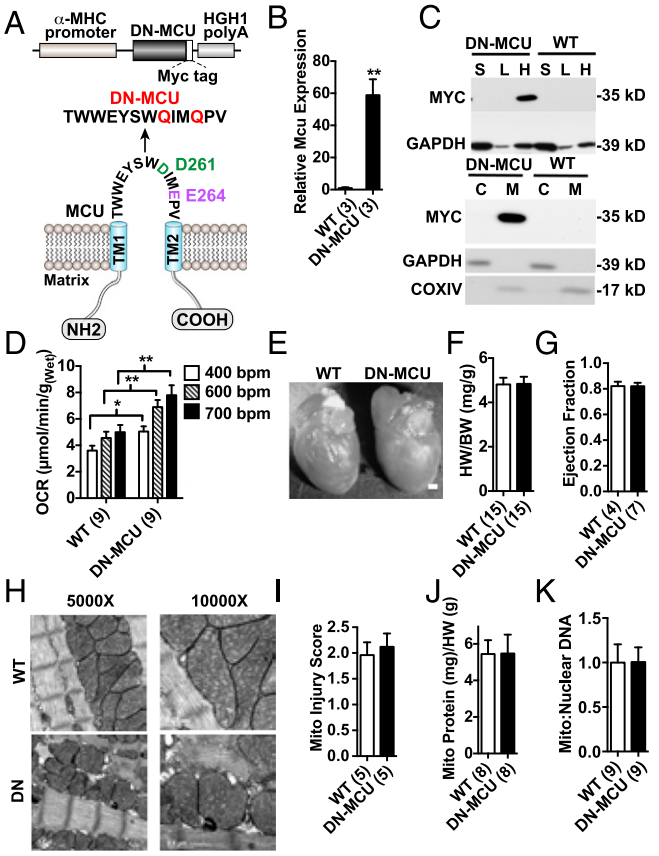


**Fig. 1.** Increased myocardial oxygen consumption in DN-MCU hearts. (*A*) Schematic of the DN-MCU construct and expressed mutant channel in the transgenic mice. (*B*) Quantitative PCR measurement for WT and DN *Mcu* transcript expression. (*C*, Top) Western blot detection of MYC-tagged protein in heart (H), liver (L), and skeletal muscle (S) tissues from DN-MCU and WT mice. GAPDH was used as a loading control. (*Bottom*) Western blot detection of MYC-tagged protein in mitochondria (M) or cytosolic (*C*) isolates from DN-MCU and WT hearts. GAPDH confirmed purity of cytosolic isolates, and COXIV confirmed purity of mitochondrial isolates. (*D*) Oxygen consumption rates in Langendorff-perfused and paced hearts (beats/min). (*E*) Representative isolated hearts. (Scale bar, 200 μm.) (*F*) Summary of heart weight (HW) to body weight (BW) ratio measurements. (*G*) Left ventricular ejection fraction measured by echocardiography in unanesthetized mice. (*H*) Representative transmission electron microscopy images (5,000× and 10,000×). (*I*) Summary data of mitochondrial injury scores. (*J*) Mitochondrial protein (mg) measurements normalized to heart weight (g). (*K*) Mitochondrial:nuclear DNA. All error bars represent SEM. $*P < 0.05$, $**P < 0.01$, Student's *t* test. Sample size (*n*) indicated for each group in parentheses.

**DN-MCU Expression Decreases Inotropic and Lusitropic Responses to Stress.** In vivo LV pressure measurements showed that DN-MCU mice had increased baseline $+dP/dt_{MAX}$ (the maximal LV pressure change rate during systole) and similar $-dP/dt_{MAX}$ compared with WT. DN-MCU mice showed reduced $\pm dP/dt_{MAX}$ responses to isoproterenol (10 μg/kg) compared with WT (Fig. S4 *A*–*F*). Based on the defect in myocardial performance in DN-MCU mice in vivo, we repeated the Langendorff-perfused heart studies under conditions suitable for measuring LV pressure. We found that DN-MCU and WT hearts had equal LV-developed pressure (LVDP) at 400 bpm, but DN-MCU hearts had significantly reduced LVDP at 600 and 750 bpm compared with WT ($P < 0.01$) (Fig. 2 *A*–*G*). DN-MCU hearts had reduced LVDP between 400 and 750 bpm ($P < 0.01$) and 600 and 750 bpm ($P < 0.05$). $+dP/dt_{MAX}$ and $-dP/dt_{MAX}$ were not different at 400 bpm, but DN-MCU hearts had diminished $\pm dP/dt_{MAX}$ responses at 600 bpm ($P < 0.01$) and 750 bpm ($P < 0.01$) (Fig. 2 *G* and *H*). The $+dP/dt_{MAX}$ was reduced in DN-MCU hearts between 400 and 750 bpm ($P < 0.01$) and 600 and 750 bpm ($P < 0.05$) and had significantly diminished $-dP/dt_{MAX}$ between 400 and 750 bpm ($P < 0.05$) (Fig. 2*I*). Under these conditions DN-MCU hearts had significantly higher OCR at 400 and 600 bpm ($P < 0.05$) (Fig. 2*J*). Within groups, OCR at 400 and 750 bpm was significantly different ($P < 0.01$) in WT, but not in DN-MCU, suggesting that DN-MCU hearts contracting against an afterload have a smaller pacing-induced OCR range than unloaded hearts.

**DN-MCU Expression Alters Mitochondrial and Cytoplasmic $Ca^{2+}$ Dynamics.** We next tested whether DN-MCU expression in ventricular myocytes prevented rapid mitochondrial $Ca^{2+}$ entry. We used

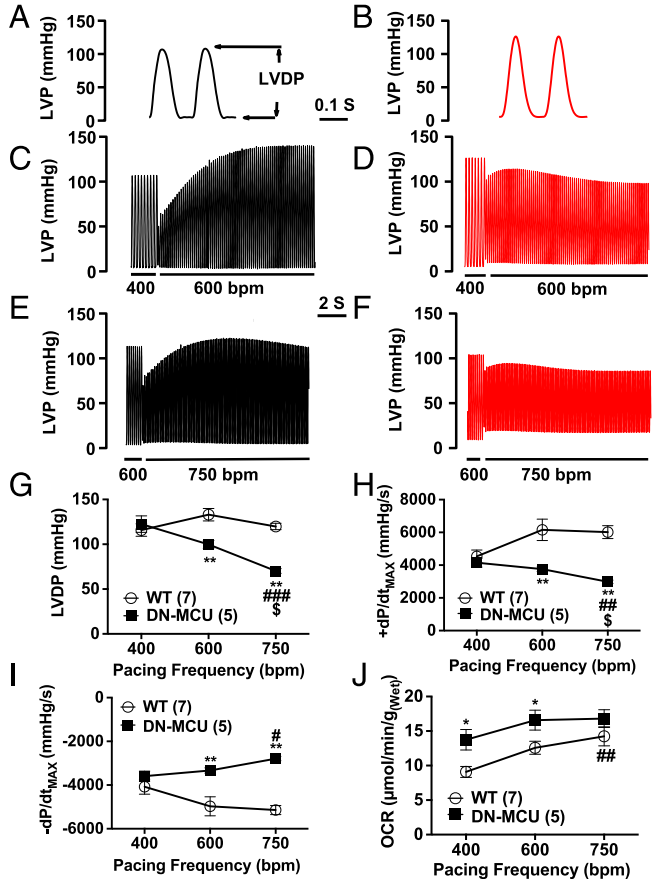


**Fig. 2.** DN-MCU expression reduced left ventricular pressure responses to pacing. (*A* and *B*) Representative waveform of left ventricular pressure (LVP) (mmHg) in WT and DN-MCU at 400 bpm, respectively. LVDP indicated by arrows. (*C* and *D*) Representative LVP changes in WT and DN-MCU hearts when increasing pacing rate from 400 to 600 bpm. (*E* and *F*) Representative LVP changes in WT and DN-MCU hearts when increasing pacing rate from 600 to 750 bpm. (*G*) LVDP (mmHg) at 400, 600, and 750 bpm. (*H*) $+dP/dt_{MAX}$ (mmHg/s) at 400, 600, and 700 bpm. (*I*) $-dP/dt_{MAX}$ (mmHg/s) at 400, 600, and 700 bpm. (*J*) OCR [µmol/min/$g_{(Wet)}$] in WT and DN-MCU hearts. All error bars represent SEM. Sample size (*n*) indicated for each group in parentheses. $*P < 0.05$, $**P < 0.01$, Student's *t* test. $\#P < 0.05$, $\#\#P < 0.01$, and $\#\#\#P < 0.001$ comparing 750 to 400 bpm; $\$P < 0.05$ comparing 750 to 600 bpm, Tukey's post hoc multiple comparison test.

freshly isolated adult ventricular myocytes with permeabilized cell membranes and incubated them with $Ca^{2+}$ green-5N (CaGr5N), a membrane-impermeable $Ca^{2+}$ sensitive fluorescent dye (3). We confirmed that DN-MCU ventricular myocytes and isolated mitochondria had complete or nearly complete loss of mitochondrial $Ca^{2+}$ uptake (Fig. 3*A* and Fig. S5*A*), similar to phenotypes observed in cells treated with the MCU antagonist Ru360 (11), lacking MCU expression (7) or expressing DN-MCU (12).

To determine if mitochondrial $Ca^{2+}$ ($[Ca^{2+}]_{mt}$) was different between DN-MCU and WT hearts, we tested $[Ca^{2+}]_{mt}$ in isolated mitochondria loaded with Fura-4FF. We found that DN-MCU mitochondria had no observable step-wise increase in Fura-4FF signal in response to repetitive $Ca^{2+}$ boluses (Fig. S5*B*). Furthermore, $Ca^{2+}$ uptake in mitochondria isolated from DN-MCU hearts was unaffected by the MCU antagonist Ru360 (Fig. S5*B*), confirming that DN-MCU expression ablated the Ru360-sensitive $Ca^{2+}$ influx. Taken together, these data show that DN-MCU myocardial mitochondria lack the MCU-mediated, rapid $Ca^{2+}$ uptake pathway.

Mitochondrial $Ca^{2+}$ stimulates pyruvate dehydrogenase phosphatase to dephosphorylate pyruvate dehydrogenase (PDH), increasing its enzymatic activity (13). We measured PDH phosphorylation in DN-MCU and WT hearts and found that PDH was significantly ($P < 0.001$) more phosphorylated (Fig. 3 *B* and *C*) and exhibited lower enzyme activity (Fig. 3*D*) in DN-MCU compared with WT cardiac mitochondria. To test whether glucose metabolism was altered in DN-MCU hearts, we used a Langendorff perfusion model with buffer containing [1,2-$^{13}C_2$]-glucose followed by NMR analysis. The $^{13}C$ incorporation was not different between groups (Fig. S6*A*), and aspartate was the only significantly increased metabolite in DN-MCU compared with WT hearts (Fig. S6 *B* and *C*). These data indicate that the lack of MCU-mediated $Ca^{2+}$ uptake in DN-MCU mitochondria is sufficient to impair activity of the $Ca^{2+}$-sensitive enzyme PDH, but without widespread changes in myocardial glucose metabolism detectable by NMR.

We next asked whether loss of mitochondrial $Ca^{2+}$ uptake would increase cytosolic $[Ca^{2+}]$ in DN-MCU cells, potentially imposing an energy demand on the sarcoplasmic reticulum/endoplasmic reticulum $Ca^{2+}$-ATPase (SERCA2a). We found significantly higher diastolic and systolic cytoplasmic $[Ca^{2+}]$ in DN-MCU cells (Fig. 3 *E*–*G*) compared with WT, suggesting that chronic MCU inhibition triggers a demand for increased SERCA activity. These findings show that chronic loss of MCU-mediated mitochondrial $Ca^{2+}$ uptake in myocardium increased OCR, possibly by enhancing the metabolic cost of cytoplasmic $Ca^{2+}$ homeostasis during excitation-contraction coupling.

We recently reported that cardiac pacemaker cells isolated from DN-MCU mice have impaired ATP production and defective cytosolic $[Ca^{2+}]$ homeostasis that was corrected by ATP dialysis (12). Based on these findings, we asked if ATP deficiency contributed to pacing-induced increases in cytoplasmic $[Ca^{2+}]$ in DN-MCU ventricular myocytes. Fortifying intracellular ATP (5 mM added to the pipette solution) significantly decreased

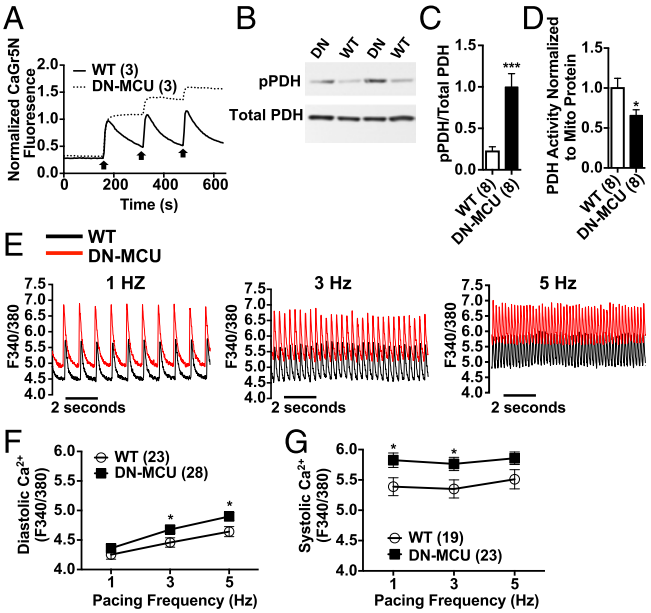


**Fig. 3.** DN-MCU expression alters cytoplasmic $Ca^{2+}$ dynamics. (*A*) Normalized kinetic tracings for CaGr5N-loaded, cell membrane-permeabilized ventricular myocytes. Arrows represent addition of 100 µM $Ca^{2+}$. (*B*) Western blot detection of phosphorylated (pPDH) and total pyruvate dehydrogenase (PDH). (*C*) Summary data for the pPDH to total PDH ratio. (*D*) Summary data for PDH activity normalized to mitochondrial protein. (*E*) Representative $Ca^{2+}$ transient traces from WT (black) and DN-MCU (red) ventricular myocytes stimulated by field stimulation. Summary data for (*F*) diastolic and (*G*) systolic $[Ca^{2+}]$ measurements made with Fura-2–loaded cells stimulated by field stimulation. All error bars represent SEM. $*P < 0.05$, $***P < 0.001$, Student's *t* test. Sample size (*n*) indicated for each group in parentheses.

cytosolic diastolic [$Ca^{2+}$] only in DN-MCU ventricular myocytes (Fig. S7 *A* and *B*). In contrast, added ATP equally and slightly decreased systolic cytosolic [$Ca^{2+}$] in WT and DN-MCU, but did not reach statistical significance (Fig. S7*C*). Taken together with findings in DN-MCU pacemaker cells (12), we interpreted these data to suggest that physiologic cytoplasmic [$Ca^{2+}$] homeostasis requires MCU-mediated ATP production.

Multiple ionic conductances may contribute to differences in cytoplasmic [$Ca^{2+}$] homeostasis between DN-MCU and WT ventricular myocytes. Therefore, we measured voltage-gated L-type $Ca^{2+}$ current ($I_{Ca}$), $Na^+/Ca^{2+}$ exchanger current ($I_{NCX}$), and sarcoplasmic reticulum $Ca^{2+}$ content (Fig. S8). We found no difference in $I_{Ca}$ (Fig. S8*A*), but $I_{NCX}$ density was increased (Fig. S8*B*) in DN-MCU cells, suggesting that DN-MCU cells partially rely on NCX to compensate for loss of MCU function. Interestingly, DN-MCU myocytes had reduced SR $Ca^{2+}$ content at baseline ($P < 0.01$) and after isoproterenol treatment ($P < 0.0001$) compared with WT (Fig. S8*C*). We interpreted these data to suggest that MCU-mediated ATP production contributes to SR $Ca^{2+}$ loading in ventricular myocytes and that MCU inhibition is accompanied by increases in $I_{NCX}$.

**No Effect of DN-MCU on OCR in Isolated Mitochondria.** Mitochondria are an important source of $O_2^{\bullet-}$ in cardiomyocytes (14) and may induce mitochondrial uncoupling to increase oxygen consumption. Therefore, we used electron paramagnetic resonance (EPR) spin trapping with the cyclic nitrone 5,5-dimethyl-1-pyrroline-N-oxide (DMPO) (15) to measure $O_2^{\bullet-}$ levels from isolated mitochondria. We found a trend ($P = 0.07$) toward less DMPO-OH signal in DN-MCU mitochondria (Fig. 4 *A* and *B*), suggesting reduced $O_2^{\bullet-}$ production. Importantly, when antimycin A, a complex III inhibitor and agent known to increase one-electron reductions of $O_2$ to form $O_2^{\bullet-}$, was included in the reaction mixture the signals from WT and DN-MCU mitochondria increased to similar peak values (Fig. 4*B*), indicating that DN-MCU and WT mitochondria have a similar capacity to produce $O_2^{\bullet-}$. Addition of superoxide dismutase (SOD) completely quenched the DMPO-OH signal in both DN-MCU and WT mitochondria, indicating that DMPO-OH was reporting on $O_2^{\bullet-}$ levels with high fidelity. These EPR data demonstrated that loss of MCU-mediated $Ca^{2+}$ entry may modestly reduce $O_2^{\bullet-}$ production in isolated mitochondria.

Excessive mitochondrial $Ca^{2+}$ entry promotes opening of the mitochondrial permeability transition pore, loss of $\Delta\Psi m$ (16), and release of mitochondrial reactive oxygen species (ROS) (17), which are consequences of ischemia-reperfusion injury that lead to myocardial death (18). We adapted our ischemia-reperfusion model to simultaneously measure $\Delta\Psi m$ and ROS in Langendorff-perfused hearts using confocal microscopy. The DN-MCU hearts maintained $\Delta\Psi m$ at baseline values during ischemic stress, whereas WT hearts showed a 19 ± 6% decrease in $\Delta\Psi m$ during ischemia compared with baseline (Fig. S9*A*), although the difference in $\Delta\Psi m$ between genotypes was not significantly different ($P = 0.12$). In the reperfusion interval, WT hearts showed increased ROS compared with DN-MCU hearts (Fig. S9*B*). Toward the end of the reperfusion interval the DN-MCU hearts had significantly reduced ROS compared with baseline ($P < 0.05$), whereas WT hearts did not show a decline in ROS relative to baseline (Fig. S9*B*). Additionally, two-way ANOVA revealed that changes in ROS during ischemia reperfusion were significantly different between DN-MCU and WT hearts ($P < 0.05$). We considered the possibility that reduced ROS in DN-MCU mitochondria could be related to increased reductive enzyme activity. To test this concept, we measured glutathione peroxidase, catalase, Cu/ZnSOD, and MnSOD in freshly isolated whole hearts and found decreased activity of MnSOD and total SOD activity (Fig. S9 *C–G*) in DN-MCU compared with WT, suggesting that the reduced ROS signal in DN-MCU hearts during ischemia reperfusion was not due to increased antioxidant enzymes. Based on an extensive body of work (16, 19, 20), we initially hypothesized that lower levels of ROS would result in myocardial protection. However, despite reduction in ROS, the DN-MCU hearts were not protected from cell death following ischemia-reperfusion injury (Fig. S9 *H* and *I*).

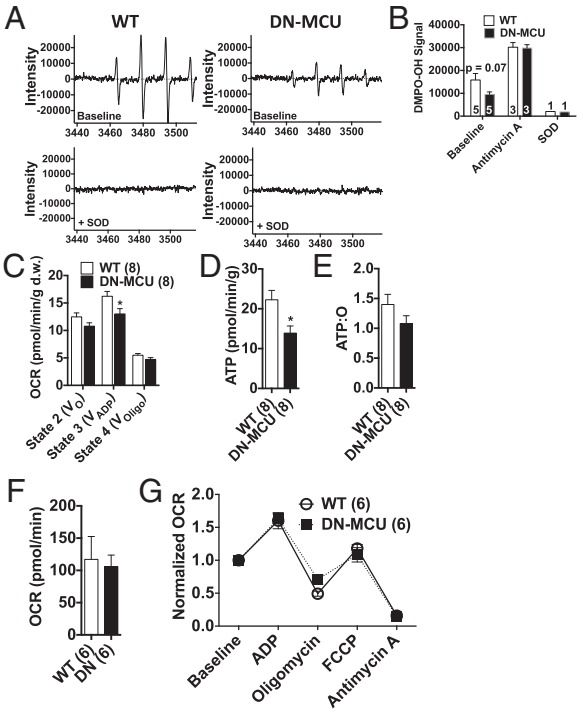


**Fig. 4.** DN-MCU mitochondria have normal OCR. (*A*) Representative electron paramagnetic resonance spectra of the DMPO-OH spin adduct produced by isolated cardiac mitochondria. (*B*) Summary showing the signal intensity of DMPO-OH baseline ($P = 0.07$, Student's *t* test) and after addition of antimycin A (1 μM) or SOD (100 U/0.5 mL). (*C*) OCR in permeabilized myocardial fibers with 156 nM $Ca^{2+}$ and 10 mM succinate in different states $V_0$ (no secondary substrate), $V_{ADP}$ (1 mM ADP), and $V_{Oligo}$ (1 mM oligomycin). Units are pmol oxygen/min/mg of dry fiber weight. (*$P < 0.05$ from WT in same state, Student's *t* test). (*D*) Bioluminescent quantification of ATP (*$P < 0.05$ Student's *t* test). (*E*) Calculated ATP:O ratios in permeabilized fibers. (*F*) Baseline OCR from isolated mitochondria without added ADP. (*G*) OCR normalized to baseline after addition of ADP (4 mM), oligomycin (2.5 μg/mL), carbonyl cyanide 4-(trifluoromethoxy)phenylhydrazone (FCCP) (4 μM), and antimycin A (4 μM). All error bars represent SEM. Sample size (*n*) indicated for each group in parentheses.

Given the increased OCR in DN-MCU hearts, we next asked whether intrinsic properties of DN-MCU mitochondria contribute to high $O_2$ consumption. First, we studied isolated permeabilized myocardial fibers (21) (bath [$Ca^{2+}$] = 156 nM) to assess OCR. We found that, in contrast to myocardium with intact cell membranes, DN-MCU fibers consumed significantly less $O_2$ than WT controls under state 3 conditions ($P < 0.05$), but had similar OCR relative to WT under state 2 and 4 conditions (Fig. 4*C*). ATP concentrations (Fig. 4*D*) were significantly lower ($P < 0.05$) in DN-MCU compared with WT samples, suggesting blunted ATP production, higher ATP hydrolysis, or both. The ratio of ATP content:$O_2$ consumption was not significantly different between DN-MCU and WT fibers (Fig. 4*E*). These findings suggest that DN-MCU mitochondria have reduced oxidative capacity compared with WT controls and are not intrinsically uncoupled, at least in the setting of membrane permeabilization and low extramitochondrial $Ca^{2+}$.

Next, we extended our findings in disrupted myocardial fibers by determining OCR in isolated mitochondria in a buffer with

nominally absent $Ca^{2+}$. At baseline, we found that isolated DN-MCU mitochondria had similar OCR to WT (Fig. 4*F*). DN-MCU and WT mitochondria responded similarly to ADP, oligomycin, FCCP, and antimycin A (Fig. 4*G*). Thus, the reduction in mitochondrial respiration in permeabilized DN-MCU fibers and isolated mitochondria in low $[Ca^{2+}]$ compared with isolated hearts suggests that extramitochondrial $[Ca^{2+}]$ contributes to the increased OCR in intact DN-MCU hearts.

**Broad Transcriptional Reprogramming in DN-MCU Hearts.** Our findings showed that inhibition of MCU has important consequences for cytoplasmic $Ca^{2+}$ homeostasis and physiological and pathological stress responses in heart. As a first step toward identifying potential transcriptional foundations for these effects, we profiled transcriptional changes induced by inhibition of MCU by performing microarray analysis to measure mRNA expression levels. We detected 636 genes with more than twofold expression change (false discovery rate < 0.05) in adult DN-MCU mice, relative to WT littermates (Fig. 5*A* and Table S1, GSE62049). Functional gene annotation clustering revealed that these genes are significantly enriched for a variety of biological processes, including acetylation, redox biochemistry, and endoplasmic nuclear signaling (Fig. 5*B*). We used qRT-PCR to measure mRNA targets from selected functional gene annotation terms and validated these targets with working primer sets (Fig. 5*C*). These data support a concept that MCU-mediated mitochondrial $Ca^{2+}$ entry has the potential to regulate transcriptional programs controlling diverse cellular pathways in myocardium. Our ANOVA analysis of mRNA expression levels revealed B-cell lymphoma 2 (*Bcl2*) to be elevated in DN-MCU samples ($P = 0.00036$). Therefore, we queried other members of the Bcl2 family and found markedly increased expression of the Bcl2-associated X protein (Bax) transcript (upregulated ninefold, $P = 0.006$, Student's $t$ test) and significantly ($P < 0.01$) elevated Bax protein expression in DN-MCU heart lysates (Fig. 5 *D* and *E*). Bax is a Bcl-2 family member implicated in mitochondrial-dependent and -independent cell death pathways (22, 23) and has been shown to impact $Ca^{2+}$ homeostasis (23), suggesting that DN-MCU hearts may have increased susceptibility to Bax-mediated death during ischemia-reperfusion injury.

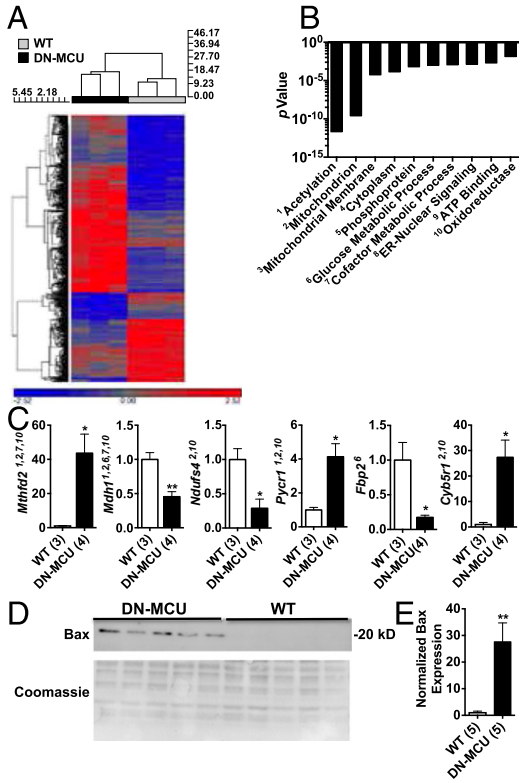


**Fig. 5.** Broad transcriptional reprogramming in DN-MCU hearts. (*A*) Hierarchical clustering of 700 differentially expressed genes (WT, black; DN-MCU, gray). (*B*) Graph shows *P* values for 10 functional terms enriched in the DN-MCU gene set. (*C*) qRT-PCR data showing validation of selected functional annotation terms listed in *B*. Superscript numbers indicate the functional annotation cluster being queried from *B*. (*D*) Western blot detecting Bax protein in whole-heart homogenates. Coomassie-stained blot shows gel loading for each sample. (*E*) Quantification of Bax Western blot (*$P < 0.05$, **$P < 0.01$, Student's $t$ test). All error bars represent SEM. Sample size ($n$) indicated for each group in parentheses.

## Discussion

We found that loss of MCU causes unanticipated cellular responses that increase OCR, disrupt cytoplasmic $Ca^{2+}$ homeostasis, and trigger transcriptional reprogramming. The ability of mitochondria to buffer cytosolic $Ca^{2+}$ is controversial (24–26). Our findings show that inhibition of MCU increases cytosolic $[Ca^{2+}]$, potentially consistent with a loss of mitochondrial $Ca^{2+}$-buffering capacity and/or ATP deficiency. We recently found that MCU inhibition limited fight-or-flight heart rate increases by lowering ATP below a critical threshold and that dialysis of 4 mM ATP was sufficient to rescue fight-or-flight responses in cardiac pacemaking cells (12). Thus, it is possible that elevated $[Ca^{2+}]$ in DN-MCU ventricular myocytes is at least partly due to inadequate ATP for physiological $Ca^{2+}$ buffering.

We observed an abrogation of OCR differences using low $[Ca^{2+}]$ buffers and when mitochondria were tested in buffers nominally lacking $Ca^{2+}$, suggesting that elevation of cytosolic $[Ca^{2+}]$ in DN-MCU hearts contributed to elevated OCR in situ. An elevated or depressed heart rate could increase or decrease OCR (27), but we controlled for this by measuring OCR at equal pacing intervals. Our in vivo data showed that DN-MCU mice had similar heart rates to WT at baseline, but an inability to increase heart rate after isoproterenol administration, consistent with recent evidence that MCU is necessary for heart rate increases during physiological stress (12). Rapid pacing in DN-MCU hearts may increase cytosolic $[Ca^{2+}]$ to a greater extent than in WT hearts due to loss of mitochondrial $Ca^{2+}$ buffering and/or inadequate ATP to sustain intracellular $Ca^{2+}$ homeostasis.

Our NMR glucose metabolite measurements did not reveal major differences in metabolites between DN-MCU and WT hearts. However, we cannot exclude the possibility that $^{13}C$ was lost as $CO_2$ through the tricarboxylic acid (TCA) cycle because we measured labeled metabolites in clamp-frozen hearts and not effluents (28). The amount of glucose uptake in paced hearts is low (29) and was below the limit of detection in our NMR studies. Thus, it is possible that DN-MCU and WT hearts had differences in glucose uptake that were undetected under these experimental conditions.

By selectively eliminating MCU activity in myocardium, our studies revealed an unanticipated feature of the interdependence of cytosolic $[Ca^{2+}]$ and oxidative phosphorylation. Elevation in cytosolic $[Ca^{2+}]$ was substantially a consequence of impaired $Ca^{2+}$-sensitive metabolism in the mitochondrial matrix because total ATP was reduced in DN-MCU hearts, compared with WT littermate controls, and because addition of exogenous ATP through a patch pipette improved cytoplasmic $[Ca^{2+}]$ in DN-MCU cardiomyocytes. To quantify the role of mitochondrial $Ca^{2+}$ buffering in sculpting cytosolic $[Ca^{2+}]$ independently of metabolic actions, it would be necessary to develop a model with matrix resident $Ca^{2+}$-activated dehydrogenases engineered for $Ca^{2+}$ insensitivity.

Our study suggests that chronic manipulation of MCU is not a viable strategy to protect cardiomyocytes from ischemia-reperfusion injury. Acute MCU inhibition has shown promise as a therapeutic

target to protect against cell death (30). We only tested for cell death in cardiomyocytes and cannot exclude the possibility that chronic MCU inhibition in different cell types could protect from pathologic stimuli. Our findings suggest that further advances in understanding mitochondrial mechanisms governing cell survival and cellular responses to loss of MCU-mediated mitochondrial $Ca^{2+}$ entry are required before developing therapies designed to prevent mitochondrial $Ca^{2+}$ overload.

## Materials and Methods

A complete description can be found in *SI Materials and Methods*.

**Mice Lacking Functional Myocardial MCU.** DN-MCU transgenic mice were recently described (12) and generated by αMHC promoter-driven expression of cDNA encoding the dominant negative form of MCU.

**In Vivo and ex Vivo Measurements.** Hemodynamic and LV pressure measurements were made in anesthetized mice with a 1-F Millar catheter and in isolated, Langendorff-perfused hearts in the presence and absence of a LV pressure transducer.

**Mitochondrial and Cytoplasmic $Ca^{2+}$, OCR, and ROS Generation.** Extramitochondrial $Ca^{2+}$ uptake was measured in cell membrane-permeabilized ventricular myocytes with CaGr5N, intramitochondrial $Ca^{2+}$ measured with Fura-FF and cytoplasmic $Ca^{2+}$ measured with Fura 2. OCR was measured in ex vivo hearts, cell membrane-permeabilized muscle fibers, and isolated mitochondria using SeaHorse Biosciences extracullular flux analyzer. $O_2^{\bullet-}$ was measured as SOD quenchable signal from isolated mitochondrial using EPR.

**ACKNOWLEDGMENTS.** We thank Dr. Elizabeth Murphy for advice and initial studies on $^{13}C$ glucose metabolism; Chantal Allamargot and the University of Iowa Central Microscopy Facility for technical assistance with electron microscopy; the University of Iowa Gene Transfer Vector Core and Mouse Transgenic Facility for technical assistance; Jinying Yang for technical support; and Kathy Zimmerman, Dr. Nathan Funk, and Dr. Tariq Hameed for echocardiographic analysis. This work was supported by National Institutes of Health Grants F30 HL114258-02 (to T.P.R.), R01 HL079031 (to M.E.A.), R01 HL070250 (to M.E.A.), R01 HL096652 (to M.E.A.), R01 HL113001 (to M.E.A.), T32 GM007337 (to University of Iowa Medical Scientist Training Program), S10 RR026293-01 (to R.M.W.), R01 DK092412 (to L.V.Z.), and R01 CA182804 (to D.R.S.). This work was supported by Veterans Administration Merit Review Program Grant 1I0BX000718 (to L.V.Z.). The Electron Spin Resonance Facility was supported in part by Holden Comprehensive Cancer Center Grant P30 CA086862.

1. Drago I, De Stefani D, Rizzuto R, Pozzan T (2012) Mitochondrial Ca2+ uptake contributes to buffering cytoplasmic Ca2+ peaks in cardiomyocytes. *Proc Natl Acad Sci USA* 109(32):12986–12991.
2. Hopper RK, et al. (2006) Mitochondrial matrix phosphoproteome: Effect of extra mitochondrial calcium. *Biochemistry* 45(8):2524–2536.
3. Joiner ML, et al. (2012) CaMKII determines mitochondrial stress responses in heart. *Nature* 491(7423):269–273.
4. Glancy B, Balaban RS (2012) Role of mitochondrial Ca2+ in the regulation of cellular energetics. *Biochemistry* 51(14):2959–2973.
5. Baughman JM, et al. (2011) Integrative genomics identifies MCU as an essential component of the mitochondrial calcium uniporter. *Nature* 476(7360):341–345.
6. De Stefani D, Raffaello A, Teardo E, Szabò I, Rizzuto R (2011) A forty-kilodalton protein of the inner membrane is the mitochondrial calcium uniporter. *Nature* 476(7360):336–340.
7. Pan X, et al. (2013) The physiological role of mitochondrial calcium revealed by mice lacking the mitochondrial calcium uniporter. *Nat Cell Biol* 15(12):1464–1472.
8. Subramaniam A, et al. (1991) Tissue-specific regulation of the alpha-myosin heavy chain gene promoter in transgenic mice. *J Biol Chem* 266(36):24613–24620.
9. Murphy E, et al. (2014) Unresolved questions from the analysis of mice lacking MCU expression. *Biochem Biophys Res Commun* 449(4):384–385.
10. Glancy B, Willis WT, Chess DJ, Balaban RS (2013) Effect of calcium on the oxidative phosphorylation cascade in skeletal muscle mitochondria. *Biochemistry* 52(16): 2793–2809.
11. Hajnóczky G, et al. (2006) Mitochondrial calcium signalling and cell death: Approaches for assessing the role of mitochondrial Ca2+ uptake in apoptosis. *Cell Calcium* 40(5-6):553–560.
12. Wu Y, et al. (2015) The mitochondrial uniporter controls fight or flight heart rate increases. *Nat Commun* 6:6081.
13. Denton RM, McCormack JG, Edgell NJ (1980) Role of calcium ions in the regulation of intramitochondrial metabolism. Effects of Na+, Mg2+ and ruthenium red on the Ca2+-stimulated oxidation of oxoglutarate and on pyruvate dehydrogenase activity in intact rat heart mitochondria. *Biochem J* 190(1):107–117.
14. Burgoyne JR, Mongue-Din H, Eaton P, Shah AM (2012) Redox signaling in cardiac physiology and pathology. *Circ Res* 111(8):1091–1106.
15. Buettner GR (1987) Spin trapping: ESR parameters of spin adducts. *Free Radic Biol Med* 3(4):259–303.
16. Baines CP, et al. (2005) Loss of cyclophilin D reveals a critical role for mitochondrial permeability transition in cell death. *Nature* 434(7033):658–662.
17. Hou T, et al. (2013) Synergistic triggering of superoxide flashes by mitochondrial Ca2+ uniport and basal reactive oxygen species elevation. *J Biol Chem* 288(7):4602–4612.
18. Nakagawa T, et al. (2005) Cyclophilin D-dependent mitochondrial permeability transition regulates some necrotic but not apoptotic cell death. *Nature* 434(7033): 652–658.
19. Wang W, et al. (2008) Superoxide flashes in single mitochondria. *Cell* 134(2):279–290.
20. Piot C, et al. (2008) Effect of cyclosporine on reperfusion injury in acute myocardial infarction. *N Engl J Med* 359(5):473–481.
21. Boudina S, et al. (2007) Mitochondrial energetics in the heart in obesity-related diabetes: Direct evidence for increased uncoupled respiration and activation of uncoupling proteins. *Diabetes* 56(10):2457–2466.
22. Wei MC, et al. (2001) Proapoptotic BAX and BAK: A requisite gateway to mitochondrial dysfunction and death. *Science* 292(5517):727–730.
23. Scorrano L, et al. (2003) BAX and BAK regulation of endoplasmic reticulum Ca2+: A control point for apoptosis. *Science* 300(5616):135–139.
24. Williams GS, Boyman L, Chikando AC, Khairallah RJ, Lederer WJ (2013) Mitochondrial calcium uptake. *Proc Natl Acad Sci USA* 110(26):10479–10486.
25. Wei AC, Liu T, Winslow RL, O'Rourke B (2012) Dynamics of matrix-free Ca2+ in cardiac mitochondria: Two components of Ca2+ uptake and role of phosphate buffering. *J Gen Physiol* 139(6):465–478.
26. Pizzo P, Drago I, Filadi R, Pozzan T (2012) Mitochondrial Ca(2)(+) homeostasis: Mechanism, role, and tissue specificities. *Pflugers Arch* 464(1):3–17.
27. Duncker DJ, Bache RJ (2008) Regulation of coronary blood flow during exercise. *Physiol Rev* 88(3):1009–1086.
28. Lopaschuk GD, Barr RL (1997) Measurements of fatty acid and carbohydrate metabolism in the isolated working rat heart. *Mol Cell Biochem* 172(1-2):137–147.
29. Tada H, et al. (2000) Myocardial glucose uptake is regulated by nitric oxide via endothelial nitric oxide synthase in Langendorff mouse heart. *Circ Res* 86(3):270–274.
30. de Jesús García-Rivas G, Guerrero-Hernández A, Guerrero-Serna G, Rodríguez-Zavala JS, Zazueta C (2005) Inhibition of the mitochondrial calcium uniporter by the oxo-bridged dinuclear ruthenium amine complex (Ru360) prevents from irreversible injury in postischemic rat heart. *FEBS J* 272(13):3477–3488.
31. Alekseev AE, et al. (2010) Sarcolemmal ATP-sensitive K(+) channels control energy expenditure determining body weight. *Cell Metab* 11(1):58–69.
32. Zingman LV, et al. (2011) Exercise-induced expression of cardiac ATP-sensitive potassium channels promotes action potential shortening and energy conservation. *J Mol Cell Cardiol* 51(1):72–81.
33. Sinaasappel M, Donkersloot C, van Bommel J, Ince C (1999) PO2 measurements in the rat intestinal microcirculation. *Am J Physiol* 276(6 Pt 1):G1515–G1520.
34. Wu Y, et al. (2009) Calmodulin kinase II is required for fight or flight sinoatrial node physiology. *Proc Natl Acad Sci USA* 106(14):5972–5977.
35. Delaglio F, et al. (1995) NMRPipe: A multidimensional spectral processing system based on UNIX pipes. *J Biomol NMR* 6(3):277–293.
36. Johnson BA, Blevins RA (1994) NMR View: A computer program for the visualization and analysis of NMR data. *J Biomol NMR* 4(5):603–614.
37. Zhan F, et al. (2002) Global gene expression profiling of multiple myeloma, monoclonal gammopathy of undetermined significance, and normal bone marrow plasma cells. *Blood* 99(5):1745–1757.
38. Puente BN, et al. (2014) The oxygen-rich postnatal environment induces cardiomyocyte cell-cycle arrest through DNA damage response. *Cell* 157(3):565–579.
39. Ahmad IM, et al. (2005) Mitochondrial O2$^{\bullet-}$ and $H_2O_2$ mediate glucose deprivation-induced stress in human cancer cells. *J Biol Chem* 280(6):4254–4263.
40. Lowry OH, Rosebrough NJ, Farr AL, Randall RJ (1951) Protein measurement with the Folin phenol reagent. *J Biol Chem* 193(1):265–275.
41. Spitz DR, Oberley LW (1989) An assay for superoxide dismutase activity in mammalian tissue homogenates. *Anal Biochem* 179(1):8–18.
42. Spitz DR, et al. (1990) Oxygen toxicity in control and $H_2O_2$-resistant Chinese hamster fibroblast cell lines. *Arch Biochem Biophys* 279(2):249–260.
43. Lawrence RA, Burk RF (1976) Glutathione peroxidase activity in selenium-deficient rat liver. *Biochem Biophys Res Commun* 71(4):952–958.